Monte Carlo simulation of phase transitions in a two-dimensional random-bond Potts model

S. Chen,[1] Alan M. Ferrenberg,[1,2] and D. P. Landau[1]
[1]*Center for Simulational Physics, The University of Georgia, Athens, Georgia 30602*
[2]*University Computing and Networking Services, The University of Georgia, Athens, Georgia 30602*
(Received 27 December 1994)

Using the "multihit" Swendsen-Wang cluster flipping method, we performed extensive Monte Carlo simulations to investigate the critical behavior of the two-dimensional (2D) eight-state random-bond Potts model. We applied finite-size-scaling techniques to extract the critical exponents for two different sets of bond strengths, from which we concluded that the transition is second order with critical exponents for both sets falling into same universality class, that of a 2D Ising model. A variation of the Lee-Kosterlitz method for determining the order of a phase transition was also applied. The double-peaked structure of the specific heat, which was found in some of the bond configurations, was also studied by simulation on periodic arrangements of strong and weak bonds.

PACS number(s): 64.60.Fr, 05.70.Jk, 75.40.Mg

I. INTRODUCTION

The effect of quenched impurities on phase transitions has been of substantial interest for many years [1–11]. One prediction about the effects of quenched bond impurities comes from the Harris conjecture [1], which states that bond randomness changes the numerical values of the critical exponents only if the specific-heat exponent α is positive. Field randomness, however, always affects the numerical values of the critical exponents [2] and can even completely eliminate the phase transitions in low-dimensional systems [4–6]. Because of this more profound effect on the transition, most early studies were interested in field randomness. Only recently has it been shown that bond randomness can also have a drastic effect on the nature of a *first-order* phase transition [6–11]. Recently, a phenomenological renormalization-group argument [9] by Hui and Berker and a rigorous proof of the vanishing of the latent heat [10] by Aizenman and Wehr came to the same conclusion that bond randomness will induce a second-order phase transition in a system that would undergo a symmetry-breaking first-order phase transition.

The purpose of our work is to provide numerical evidence for this prediction by large-scale Monte Carlo simulations. The nature of the phase transition in the two-dimensional pure Potts model [12] has been known to be first order for $q>4$ and continuous for $q\leq 4$ [13], which suggests that the two dimensional q-state Potts model with $q>4$ might be eligible for testing this prediction. In Secs. II and III we first introduce the random-bond Potts model [12] and methods for simulations, followed by a brief description of the data analysis techniques. In Sec. IV we then present and discuss the results obtained from finite-size-scaling techniques [14] and the Lee-Kosterlitz method [15]. A summary is given in Sec. V. A study of the double-peaked structure of some thermodynamic quantities for a system with a periodic arrangement of different bond strengths is described in the Appendix.

II. THE RANDOM-BOND POTTS MODEL

The q-state Potts model [12] can be described by the Hamiltonian

$$-\beta H=\sum_{\langle i,j\rangle} K_{ij}\delta_{\sigma_i,\sigma_j}\ , \tag{1}$$

where $\beta=1/k_BT$. The spin σ can take the values $1,2,\ldots,q$ and δ is the Kronecker delta function. The sum runs over all nearest-neighbor bonds in the system and K_{ij} is the dimensionless interaction between σ_i and σ_j. In a pure system, K_{ij} is constant for all bonds and the value of the transition temperature is known for all q as are the critical exponents for $q\leq 4$ [12]. The random-bond Potts model (RBPM) discussed by Wu [12] is described by the above Hamiltonian with the couplings K_{ij} randomly selected from two ferromagnetic couplings K_1 and K_2 according to the distribution

$$P(K)=p\delta(K-K_1)+(1-p)\delta(K-K_2)\ . \tag{2}$$

For a system with $p=0.5$, the system is self-dual and the exact critical value of K_1 and K_2 can be derived by duality relations [16]. This has been done by Kinzel and Domany and is given by the implicit equation [17]

$$(e^{K_1^C}-1)(e^{K_2^C}-1)=q\ , \tag{3}$$

where K_1^c and K_2^c are the corresponding values of K_1 and K_2 at the transition. For the rest of this paper, we will discuss this model in terms of the ratio of the strong coupling to the weak one $r=K_2/K_1$ and K_1 will be our temperaturelike variable. In the simulations we chose $q=8$, which is known to have a strong first-order transition, in the hope that we would not have too much trouble in determining the order of the transition in the random-bond system. We also avoided choosing q larger than 8 in the hope that we could observe the asymptotic behavior without needing very large systems.

For a system with quenched randomness, the fluctuation of the thermodynamic quantities is large for different

bond distributions so configurational averaging over randomness is necessary to produce a correct result. To minimize the number of bond configurations needed for the averaging, we confined our study to bond distributions in which there are the same number of strong and weak bonds in each of the two lattice directions. This procedure should reduce the variation between different bond configurations, but we expect that this restricted version of the random-bond Potts model will have similar behavior in the thermodynamic limit.

III. METHODS

A. The multihit Swendsen-Wang algorithm

Near a phase transition, traditional (single-flip) Monte Carlo algorithms suffer from critical slowing down. Cluster flipping methods [18] can greatly reduce the correlation time; however, they are quite slow, in terms of the amount of CPU time needed per spin compared to vectorized and/or multispin coding single spin-flip algorithms. In order to increase the speed we developed a "multihit" approach [19], based on the Swendsen-Wang (SW) method [20], which can be substantially faster than SW updating depending on the particular model being simulated.

A SW simulation algorithm has three main procedures: (i) Find and label clusters in a bond configuration. (ii) "Decorate" clusters by assigning a new Potts variable to each cluster. (iii) Make measurements. In considering the efficiency of the SW algorithm one must make two points. First, cluster finding [step (i)] is the most time consuming part of the algorithm in spite of attempts made to speed it up, by vectorization or parallelization [21]. Second, only one decoration [step (ii)] is chosen out of a total number q^{N_C} possible choices, where N_C is the number of clusters present in a cluster configuration. (Each of the N_C clusters is independent of the others in the random cluster representation and is randomly assigned one of the q states. Therefore, there are q^{N_C} distinct decorations for each cluster configuration.) The idea behind the multihit SW algorithm is to take advantage of this large number of possible decorations of the cluster configuration by choosing more than one decoration ("hit") per cluster configuration. In other words, a multihit method repeats steps (ii) and (iii) multiple times after step (i).

Let t_{cluster}, t_{decorate}, and t_{measure} represent the time needed for each step respectively. The time per measurement for a SW update is given by

$$t_{\text{SW}} = t_{\text{cluster}} + t_{\text{decorate}} + t_{\text{measure}} .$$

In the multihit algorithm each cluster configuration is decorated n times resulting in n spin configurations and n measurements. The time per measurement of an n-hit update is therefore

$$t_{\text{MHSW}}(n) = \frac{t_{\text{cluster}}}{n} + t_{\text{decorate}} + t_{\text{measure}} .$$

The speedup of the algorithm is given by the ratio $t_{\text{SW}}/t_{\text{MHSW}}$

$$\frac{t_{\text{SW}}}{t_{\text{MHSW}}(n)} = \frac{R+1}{R/n+1} ,$$

where $R = t_{\text{cluster}}/(t_{\text{decorate}} + t_{\text{measure}})$. As this ratio always ≥ 1, the time consuming step of finding the clusters is effectively eliminated for large n; however, the increase in speed depends on the particular model being studied as well as the particular computer used and the implementation of the algorithm since the time needed to find the clusters depends on both the size distribution of the clusters as well as the shapes of the clusters. For the two-dimensional (2D) Ising model ($q=2$ Potts model) with a program implemented on an IBM RS/6000 workstation, the ratio of t_{decorate} to t_{cluster} is 0.074 while the ratio of t_{measure} to t_{cluster} is 0.08, which yields $R=6.5$; for the 2D eight-state $r=10$ random-bond Potts model, these ratios are 0.26 and 0.43, respectively, yielding $R=1.45$; for the $r=2$ RBPM, the ratios are 0.35 and 0.43; thus $R=1.28$.

To determine the efficiency of the multihit approach, we must also consider the correlation time for the algorithm. If the number of independent measurements (per unit time) is given by

$$N(n) = \frac{1}{t_{\text{MHSW}}(n) \times [2\tau_{\text{MHSW}}(n)+1]} ,$$

where τ_{MHSW} is the integrated autocorrelation time, the true efficiency of the multihit method, relative to the single-hit (SW) algorithm, is

$$N(n)/N(1) = \frac{(1+R)}{(1+R/n)b(n)} ,$$

where $b(n)$ is $[2\tau_{\text{MHSW}}(n)+1]/[2\tau_{\text{MHSW}}(1)+1]$. For an eight-state Potts model with linear size $L=64$, the integrated correlation time for the SW algorithm [equivalent to the $n=1$ multihit SW (MHSW) algorithm] is approximately 5000 Monte Carlo steps (MCS) for the pure system, 400 MCS for $r=2$, and 25 MCS for $r=10$. For n hits, the correlation time varied from $\sim 0.8n\tau_{\text{MHSW}}(1)$ to $\sim n\tau_{\text{MHSW}}(1)$, depending on the bond configuration. Therefore, the relative efficiency of the multihit algorithm with three hits is ~ 0.7 for the random-bond Potts model and 1.1 for the 2D uniform-bond Ising model.

In terms of the number of independent measurements per second, the SW algorithm is still more efficient than MHSW. However, it has recently been shown, for studies that use histogram techniques [22,23], that it may be advantageous to generate additional measurements, even if these are correlated [24]. This is illustrated by Fig. 1, in which we compare the K_1 dependence of the measured statistical error in the energy for the two algorithms, using the same amount of CPU time. The simulations were performed at the infinite-lattice transition point for the $r=2$ random-bond Potts model. From an examination of Fig. 1 we see that the MHSW algorithm actually has a smaller relative error over a wider range of coupling constant K_1 than does the SW algorithm. Therefore, the MHSW algorithm can give us reliable information over a larger range of K_1 to help us locate peaks in thermodynamic functions.

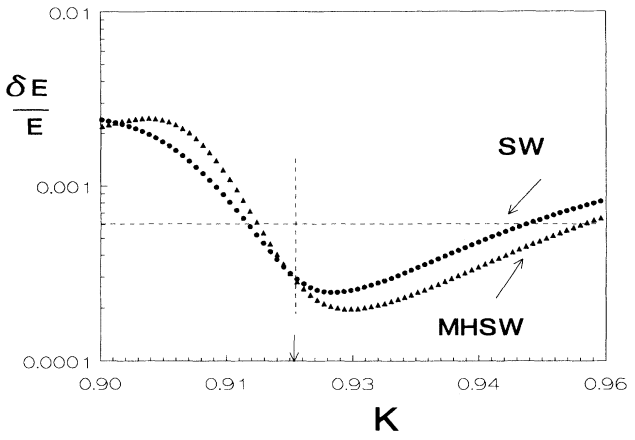

FIG. 1. Comparison of the relative error in E determined by SW and MHSW simulation for the $r=2$ random-bond Potts model. The simulations were performed at infinite-lattice transition point (0.920 185) shown by the arrow. The horizontal line represents 6×10^{-4} relative standard error.

A further advantage of the multihit SW algorithm is that it is easy to implement on a distributed memory parallel computer. A successful parallel version of the multihit SW algorithm has been developed using the Parallel Virtual Machine (PVM) [25]. The efficiency $(N_{\rm PVM})/(N_{\rm SW}\times$number of processors) of this parallel algorithm is ~0.75 with two processors and three hits on each processor.

B. Reweighting and configurational averages

Histogram techniques, which are used to increase the amount of information obtained from a Monte Carlo study, have been applied successfully to the study of critical phenomena [26,27]. Detailed descriptions of the histogram techniques used in this study have been presented elsewhere [22,23]; here we only briefly describe the method. In these methods the histogram $H(E,M)$ for a given simulation coupling K_0 of dimensionless energy E and magnetization M kept during the simulation is reweighted to provide an estimate for the equilibrium probability distribution $P_K(E,M)$ at any K. The average value of any function of E and M, $A(E,M)$, can then be calculated as a continuous function of K

$$\langle A(E,M)\rangle(K)=\sum_{E,M}A(E,M)P_K(E,M)\ . \tag{4}$$

The average of a function with mixed terms such as E^nM^m can be expressed by

$$\langle E^n f(M)\rangle(K)=\frac{\sum_E E^n\langle f\rangle_E P_K(E)}{\sum_E P_K(E)}\ , \tag{5}$$

where $P_K(E)=\sum_M P_K(E,M)$ and $\langle f\rangle_E$ is the constant energy average of $f(M)$ estimated from the simulation data. The computer memory requirements are thus greatly reduced. We have used the simulation data to construct the one-dimensional histogram $H(E)$ $[=\sum_M H(E,M)]$ as well as four constant-E averages $\langle M\rangle$, $\langle M^2\rangle$, $\langle M^3\rangle$, and $\langle M^4\rangle$. We then calculated $P_K(E)$ from $H(E)$ and all of the necessary thermodynamic quantities were calculated by using Eq. (5).

For a system with randomness, the configurational average over randomness is necessary for obtaining correct bulk properties. The configurational average value of a thermodynamic function is obtained by first calculating the reweighted average $\langle A\rangle$ [Eq. (4)] for a given bond configuration, summing up $\langle A\rangle$ for all bond distributions, then dividing by the total number of bond configurations N_σ,

$$[\langle A\rangle]=\frac{\sum_{i=1}^{N_\sigma}\langle A\rangle_i}{N_\sigma}\ , \tag{6}$$

where $[\langle A\rangle]$ represents the configurational average of $\langle A\rangle$. As $\langle A\rangle$ is a continuous function of K, so is its configurational average $[\langle A\rangle]$. The maximum value for any thermodynamic quantity such as $C_{\rm max}$ and $\chi_{\rm max}$ used in the finite-size-scaling analysis is just the maximum of the configurational average

$$A_{\rm max}=[\langle A\rangle]_{\rm max}\ . \tag{7}$$

C. Finite-size scaling and Lee-Kosterlitz method

Finite-size-scaling theory [29] is a traditional and powerful method for studying second-order phase transitions and also provides a way to determine the order of the transition. The principal statement of the finite-size-scaling formalism is that the finite-size rounding and shifting of critical singularities are controlled by the ratio between the correlation length ξ and the linear dimension L of the system [29]. The singular part of the free energy of a system that undergoes a second-order transition is given by

$$F(L,T,h)=L^{-(2-\alpha)/\nu}\mathcal{F}(tL^{1/\nu},hL^{(\gamma+\beta)/\nu})\ , \tag{8}$$

where $t=(T-T_C)/T_C$ (T_C is the infinite-lattice critical temperature). The critical exponents α, β, γ, and ν are all the appropriate values for the infinite system. The various thermodynamic properties (for $h=0$) can be determined from the above equation and have corresponding scaling forms, e.g.,

$$C_{\rm max}\sim L^{\alpha/\nu}\mathcal{Z}(tL^{1/\nu})\ , \tag{9}$$

$$\chi_{\rm max}\sim L^{\gamma/\nu}\mathcal{X}(tL^{1\nu})\ , \tag{10}$$

$$K_c(L)=K_c+\lambda' L^{-1/\nu}\ . \tag{11}$$

These expressions will be modified by corrections to scaling and corrections to finite-size scaling [27,30]. Since the introduction of each additional term adds two more parameters in a nonlinear fit, thus requiring far more accurate simulation data, we combined these corrections into a single term with an effective exponent w. The size dependence of the critical coupling K_c becomes

$$K_c(L)=K_c+\lambda' L^{-1/\nu}(1+b'L^{-w})\ . \tag{12}$$

It has recently been shown that other, less traditional, quantities can be used effectively in finite-size-scaling analyses [27]. For example, the maxima of logarithmic derivatives of any power of the order parameter M

$$\frac{\partial \ln\langle M^n\rangle}{\partial K_1}=\frac{1}{\langle M^n\rangle}\frac{\partial\langle M^n\rangle}{\partial K_1}=\frac{\langle M^n E\rangle}{\langle M^n\rangle}-\langle E\rangle\ , \tag{13}$$

and the derivative of the fourth-order magnetization cumulant $\partial U_B/\partial K_1$, where

$$U_B=1-\frac{\langle (M-\langle M\rangle)^4\rangle}{3\langle (M-\langle M\rangle)^2\rangle^2}\ , \tag{14}$$

scale with system size as $L^{1/\nu}$, which allows us to directly calculate ν. In addition, these quantities provide further estimates of finite-size transition couplings.

Finite-size effects at first-order transitions have begun to receive attention comparatively recently [28–41]. According to the proposal of Fisher *et al.*, the singular part of the free energy for a system with periodic boundary conditions undergoing a first-order phase transition [31,32] can be written as

$$F(L,T)=L^{-d}\mathcal{F}(tL^d) \tag{15}$$

and the scaling forms for various thermodynamic quantities are

$$\chi_{\max}\sim L^d\chi(tL^d)\ , \tag{16}$$

$$C_{\max}\sim L^d\mathcal{C}(tL^d)\ , \tag{17}$$

$$K_c(L)=K_c+\lambda' L^{-d} \tag{18}$$

The qualitative theory of finite-size scaling at a temperature-driven first-order phase transition was derived in [34] and [35] by using double Gaussian probability distributions for the energy.

Several methods have been proposed to distinguish numerically between continuous and first-order transitions [15,36–39]. One of these approaches [15] is due to Lee and Kosterlitz, who suggest that the size dependence of the free energy as a function of energy

$$F_L(E)=-\ln P_L(E)\ , \tag{19}$$

where $P_L(E)$ is the probability distribution for a system of linear dimension L, can be used to umambiguously identify a weak first-order transition [42] even when the system size is smaller than the correlation length. Their technique makes use of the fact that for large systems the free energy at a first-order phase transition will consist of two minima of equal depth separated by a peak. (The probability distribution will therefore have two maxima separated by a minimum.) If the free-energy barrier (difference between the minima and the peak) grows with increasing system size, the transition will be first order in the thermodynamic limit; otherwise, the transition will be second order. In Monte Carlo simulations, the free-energy barrier can be estimated by reweighting the energy histogram [22]

$$\Delta F=\ln\frac{P_L(E_1)}{P_L(E_2)}=\ln\frac{H(E_1)}{H(E_2)}+(K_C-K_0)(E_1-E_2)\ , \tag{20}$$

where E_1 and E_2 are the energies at which $P_L(E_1)$ and $P_L(E_2)$ have the maximum and the minimum value, respectively. We have used a variation of this approach to apply to the random system since in such a system a configurational average over randomness is necessary. We reweighted the histograms [22,23] until the two peaks have the same height (this defines the K_C), then calculated the free-energy barrier using Eq. (20) for the given bond configuration. We then performed the configurational average over bond distributions [Eq. (6)] to extract the final probability distribution and free-energy barrier.

IV. RESULTS AND DISCUSSIONS

We have performed simulations of the eight-state Potts model with periodic boundary conditions. The strong to weak bond ratios $r\ (=K_1/K_2)$ were chosen to be integers for the convenience of establishing histograms. The simulations were performed, using the MHSW algorithm, on a cluster of IBM RS/6000 workstations. Part of the simulations were carried out with MHSW algorithm implemented using PVM. The number of hits was chosen as 10 and 5 in each of the two sets of simulations respectively. The first set of simulations, having the weakest randomness ($r=2$), was done for linear size $12\le L\le 128$. Some preliminary results for $r=2$ have been presented elsewhere [43]. Data were taken near the corresponding infinite lattice transition coupling obtained from Eq. (3) ($K_1^C=0.920\,185\,27\ldots$). Between 6×10^5 and 1.5×10^6 Monte Carlo steps (complete lattice updates) were performed for each simulation, which was always more than 10^2 times the correlation time. For a given bond configuration, we performed five independent simulations at the same temperature and applied the single-histogram method [22] to find the position ($K_{C_{\max}}$) of the maximum value of the specific heat. This procedure was repeated until the change in $K_{C_{\max}}$ was smaller than the statistical error of the simulations. Up to 40 different bond distributions were simulated for each size and the configurational average was performed over these bond distributions by using Eq. (6).

Another set of simulations was performed for $r=10$ to investigate the effect of a different bond ratio. The infinite-lattice transition coupling K_1^C for $r=10$ is $0.312\,655\,66\ldots$. The simulations were done for linear size $24\le L\le 84$, with a run length of 10^6 Monte Carlo steps for each simulation, which was at least 10^4 times the correlation time. In the first stage, we simulated 30 bond configurations for each linear size up to $L=48$, using the single-histogram technique for the analysis. The locations of the specific-heat peaks for some of the bond configurations fluctuated over a wide range of couplings. With some extra simulations, we used the multiple histogram method to analyze the specific heat for some of these "problem" bond configurations. The result showed that the specific heat had *two peaks* for these bond configurations. To help understand the origin of the double-peaked structure in the specific-heat, we performed a systematic study on systems in which strong

and weak bonds are arranged periodically. The results are given in the Appendix. Although the specific heat of some of the bond configurations has two peaks, the specific heat resulting from the configurational average has only one peak for all system sizes.

We then performed simulations, over a wide range of couplings, for all bond configuration using 10–30 couplings for L up to 48 and 10–15 for $L=64$. For each lattice size ($28 \leq L \leq 64$), a total of 150–200 bond configurations were simulated; only 60 for $L=24$. The multiple-histogram technique [23] was used in obtaining the average value of the thermodynamical functions. As in the analysis of $r=2$, the configurational average was then taken by using Eq. (6).

For $L=84$, the simulations were performed only around the expected locations of the specific-heat peak as estimated from finite-size scaling. A total of 200 bond configurations were simulated.

A. Results for the free-energy barrier

The energy distributions from some bond configurations for $r=2$ have two peaks, which can be an indication of a first-order transition. However, the percentage of double-peaked distributions decreases with increasing system size. We applied the Lee-Kosterlitz method to analyze the energy histograms to determine the order of phase transition. The resultant free-energy barrier $\Delta F(L)$ is plotted as a function of inverse lattice size in Fig. 2. The trend for large L is toward zero free-energy barrier, which indicates that the transition has indeed changed from first to second order. For the uniform eight-state Potts model, the analytical value of the free-energy barrier [44] is $0.083\,758L$, which is significantly larger [$\Delta F(L=16) \approx 1.3$] and grows with increasing system size. Note that for smaller L the trend toward $\Delta F=0$ is not as clear, indicating that these systems may not yet be in the asymptotic regime. We also investigated the energy histograms for $r=10$, but found that there was only one peak in the energy distribution for $L \geq 24$, which strongly suggests that the transition is second order.

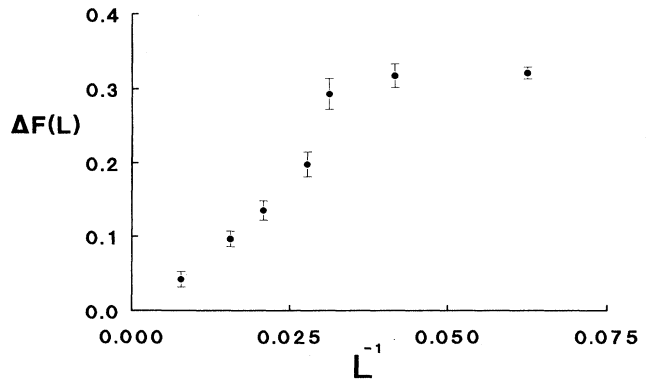

FIG. 2. Plot of the free-energy barrier $\Delta F(L)$ for $r=2$ as a function of inverse lattice size.

B. Finite-size-scaling results for $r=2$

In applying the finite-size-scaling techniques, we first determine the critical exponent ν. Several thermodynamic quantities can be used to obtain ν from Monte Carlo simulation data. The scaling behavior of the derivative of Binder's fourth-order cumulant U_B is one example. However, the locations of the peaks of the derivative of U_B were too far from the couplings used for the simulations, which were near the specific-heat peaks, to allow accurate single-histogram technique reweighting. In this study, we investigated the scaling behavior of the logarithmic derivatives of M, M^2, and M^4 to determine the critical exponent ν.

In previous studies of the Potts model, the quantity

$$M=\frac{q\rho-1}{q-1}\ , \tag{21}$$

where $\rho=L^{-d}\max(M_1,M_2,\ldots,M_q)$ and M_i is the number of spins in state i, has been used as an order parameter [35], although it does not exhibit the full symmetry of the model. In the early stages of this work [43] we kept and used microcanonical averages for $\langle\rho\rangle$, $\langle\rho^2\rangle$, and $\langle\rho^4\rangle$ rather than $\langle M\rangle$, $\langle M^2\rangle$, and $\langle M^4\rangle$. We corrected the results for the logarithmic derivatives of $\langle M\rangle$ and $\langle M^2\rangle$ for this paper, but because we did not keep $\langle\rho^3\rangle$, we were unable to correct the results for $\langle M^4\rangle$ and the cumulant U_B. We found, however, that the exponents determined with the "incomplete" order parameter actually agree well with the "correct" results.

In Fig. 3 we plot these logarithmic derivatives as a function of system size on a log-log scale. The solid lines represent linear fits for $L \geq 24$. We have the values of ν listed in Table I. Combining these results we get a final value $\nu=1.004\pm0.019$. Within errors, this agrees with the $d=2$ Ising model value $\nu=1$. For the range of system sizes in this study, we could see no indication that

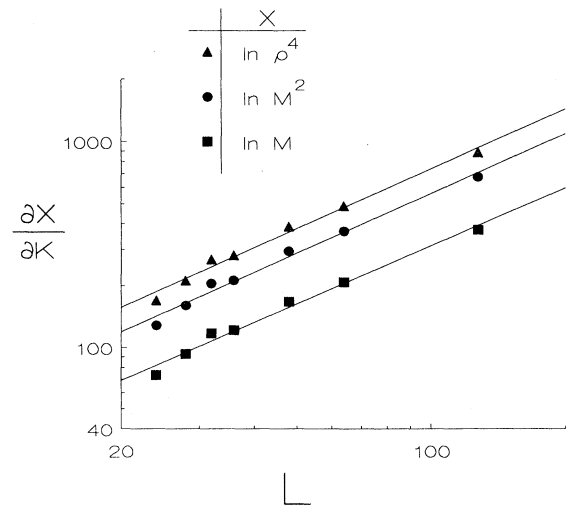

FIG. 3. log-log plot of the size dependence of logarithmic derivatives of the order parameter of $r=2$. The solid lines are linear fits including systems with $L \geq 24$. Errors in the individual points are comparable to the symbol size.

TABLE I. Fitted values of ν for the logarithmic derivatives of M, M^2, and ρ^4 for bond strength ratio $r=2$.

Derivative	ν	Error
M	1.015	0.036
M^2	1.000	0.032
ρ^4	0.998	0.030

first-order behavior will appear for large L (although, of course, we cannot exclude this possibility). We therefore conclude that the additional of bond randomness has changed the order of the phase transition from first to second.

As a further test of the $d=2$ Ising-like critical behavior, we examined the specific-heat critical exponent α. The critical behavior of the specific-heat in a 2D Ising model has a logarithmic size dependence, i.e.,

$$C_{\max}(L)=a+b\ln L \ . \tag{22}$$

We plotted the specific-heat maxima as a function of lattice size on a semilogarithmic scale. The result, shown in Fig. 4, indicates that the data can be well described by a linear fit (the solid line), with background term $a=-42.6$ and a goodness of fit of 0.90, for systems larger than $L=28$ as would be expected for a two-dimensional Ising model. Fitting the specific heat to a power law yields $\alpha/\nu=0.02\pm0.20$, with a background term -1252.5 and a goodness of fit of 0.86. The fact that the quality of the fit is about the same indicates that it hard to distinguish a small power-law divergence from a logarithmic one. It is clear, however, that the divergence of the specific heat is significantly slower than the L^2 expected for a first-order transition.

We also studied the location of the peaks in other thermodynamic functions. Those peaks occurred at different values of $K_1^c(L)$, but all of the positions moved toward larger K as the lattice size increased. A contour plot has been made to investigate the global χ^2 minimum from a general linear least-squares fitting using Eq. (12). With

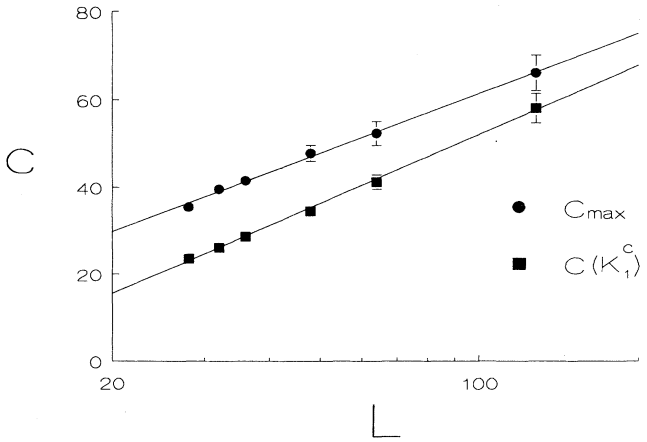

FIG. 4. Semilogarithmic plot of the specific heat vs lattice size for the maximum value of the specific heat for $r=2$ as well as the specific heat at the infinite critical point $K_1^c(r=2)$. The solid lines are linear fits including data for $L\geq 28$. Where not shown, error bars are smaller than the symbol sizes.

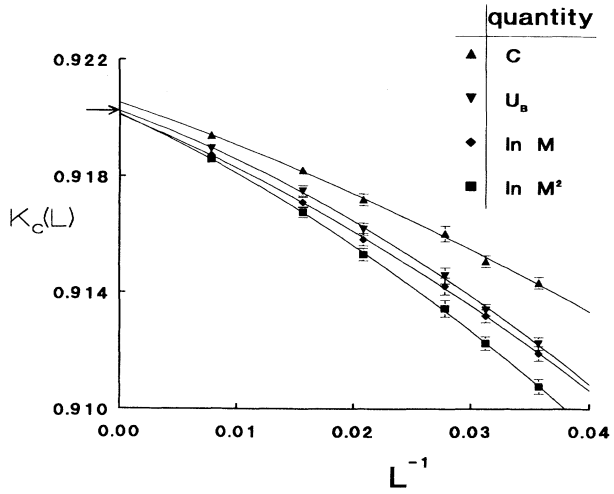

FIG. 5. Size dependence of the estimates for finite-lattice critical couplings $K_1^c(r=2)$ for various thermodynamic quantities. The solid curves are fits to the finite-size-scaling form including the lowest-order correction term [see Eq. (13)]. The arrow shows the location of the exact transition points 0.920 185.

$\nu=1$, the minimum of χ^2 occurred at around $w=1$. Using the 2D Ising value $\nu=1$ and a correction term with $w=1$, we fitted the positions of the maxima using Eq. (12). The result, plotted in Fig. 5, showed that for $L\geq 28$ all of the positions can be well fitted with an extrapolated value $K_c=0.9202\pm0.0003$, in excellent agreement with the "exact" value $K_{1c}=0.920\,185\,27\ldots$, quoted earlier. Table II is a collection of the extrapolated values for various quantities.

The analysis of the behavior of the moments of the order parameter at K_c gives us an estimate for β. The result for β/ν, determined by the scaling behavior of M at K_C, is 0.118 ± 0.008, while the value of $2\beta/\nu$, determined from M^2, is 0.247 ± 0.006. Both of these are in agreement with the $d=2$ Ising model values (0.125 and 0.25, respectively).

C. Finite-size-scaling results for $r=10$

We first analyzed the scaling properties of the magnetic susceptibility, the maximum values of which have smaller fluctuations than most other thermodynamic quantities. The result is shown in Fig. 6, where we plot the magnetic susceptibility maximum as a function of lat-

TABLE II. Infinite transition couplings extrapolated from the locations of the maximum value of various quantities for bond strength ratio $r=2$.

Quantity	K_1^c
$\frac{\partial U_B}{\partial K_1}$	0.9202
$\frac{\partial \ln M}{\partial K_1}$	0.9201
$\frac{\partial \ln M^2}{\partial K_1}$	0.9201
$C_{\max}$	0.9204

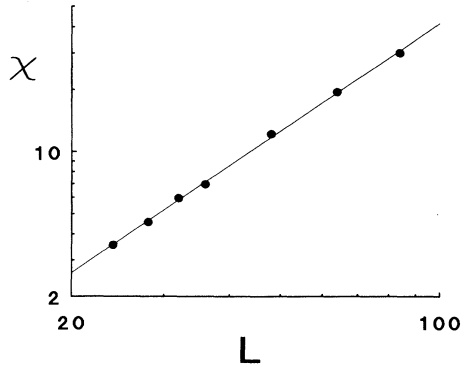

FIG. 6. log-log plot of the size dependence of maximum value of the susceptibility for $r=10$. The solid line is linear fit including systems with $L \geq 28$. Errors in the individual points are smaller than the symbol size.

tice size on a log-log scale. The value of γ/ν, the slope of the linear fit (solid line), is

$$\gamma/\nu = 1.72 \pm 0.03 \ . \tag{23}$$

From the analysis of the moments of the order parameter M and M^2 at K_1^C we obtained

$$\beta/\nu = 0.126 \pm 0.013 \tag{24}$$

and

$$2\beta/\nu = 0.258 \pm 0.023 \ . \tag{25}$$

From the scaling and hyperscaling laws

$$\alpha + 2\beta + \gamma = 2 \ , \tag{26}$$

$$\alpha + d\nu = 2 \ , \tag{27}$$

we would estimate $\alpha = 0.02 \pm 0.05$ and $\nu = 0.99 \pm 0.05$. All these exponents are consistent with the $d=2$ Ising model values.

As in the analysis for $r=2$, we investigated the logarithmic behavior of the specific heat. Despite the double-peak structure of the specific heat in some of the bond configurations, the configurational average has only

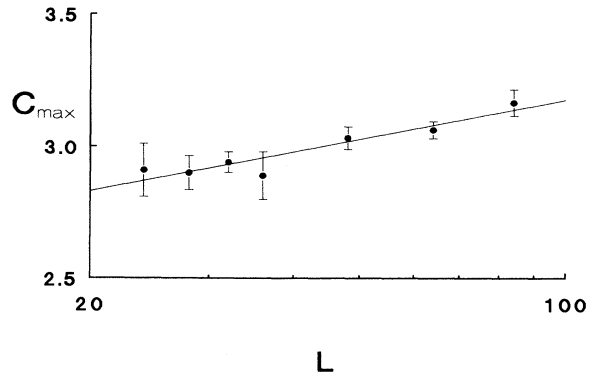

FIG. 7. Semilogarithmic plot of the maximum value of the specific heat of $r=10$ vs lattice size. The solid line is a linear fit including data for $L \geq 28$.

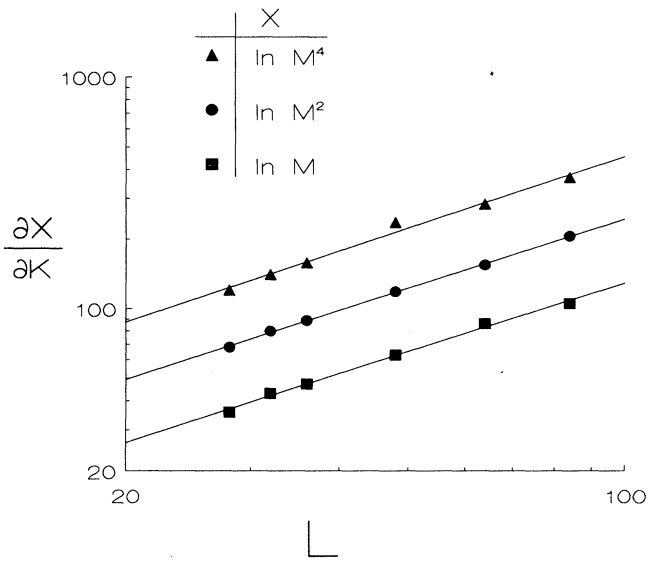

FIG. 8. Log-log plot of the size dependence of logarithmic derivatives of the order parameter of $r=10$. The solid lines are linear fits including systems with $L \geq 28$. Errors in the individual points are comparable to the symbol size.

one peak. (A systematic study of the double-peak structure in specific heat is included in the Appendix.) Figure 7 shows a semilogarithmic plot of the maxima of the specific heat as a function of lattice size. The linear fit for $L \geq 28$ (the solid line) gives a background term 2.17 and a goodness of fit 0.86.

Further confirmation comes from the scaling behavior of the logarithmic derivatives of M, M^2, and M^4. In Fig. 8 we plot these logarithmic derivatives as a function of system size on a log-log scale. The values of ν obtained from the linear fit (solid lines) are listed in Table III. Combining these results we obtain $\nu = 1.02 \pm 0.02$, again, in agreement with the 2D Ising value within errors.

As a final confirmation of 2D Ising-like critical exponents, we fitted the positions of the maxima using the 2D Ising value $\nu=1$ and a correction term $w=1$ (around which the minimum of χ^2 occurred). The result, plotted in Fig. 9, shows that for $L \geq 28$ all the positions could be well fitted with the extrapolated value of $K_C = 0.3126 \pm 0.0008$, which also agrees with the exact value (0.312 655 . . .).

V. SUMMARY

We have studied the effects of quenched bond randomness in the eight-state Potts model. The result of rather

TABLE III. Fitted values of ν for the logarithmic derivatives of M, M^2, and M^4 for bond strength ratio $r=10$.

Derivative	ν	Error
M	1.04	0.04
M^2	1.03	0.03
M^4	1.00	0.04

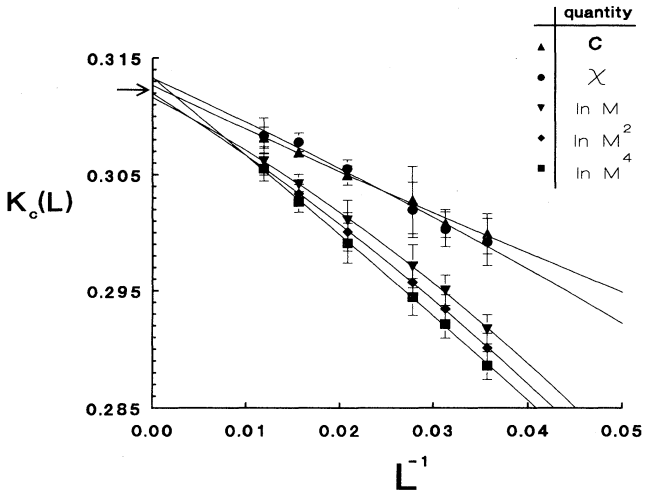

FIG. 9. Size dependence of the estimates for finite-lattice critical couplings $K_1^c(r=10)$ for various thermodynamic quantities. The solid curves are fits to the finite-size scaling form including the lowest-order correction term [see Eq. (12)]. The arrow shows the location of the exact transition point.

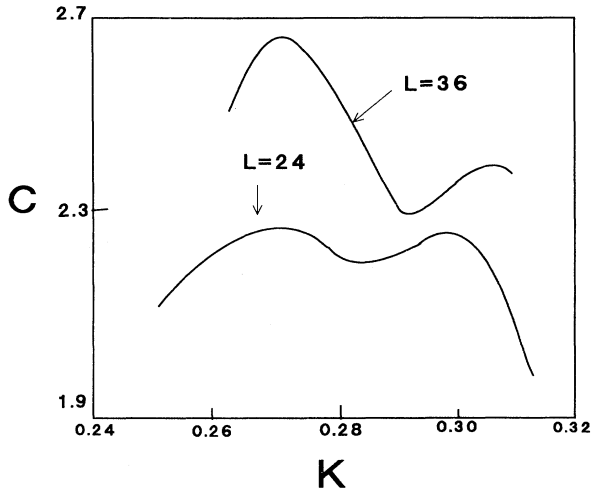

FIG. 10. Plot of an example of the double-peaked structure for $r=10$ random-bond configurations.

extensive simulations for the $q=8$ Potts model with two sets of randomly distributed ferromagnetic bonds of two different strengths is that a second-order transition with 2D Ising exponents results. To significantly improve these results would require at least an order of magnitude more computer time ($\sim 10\,400$ h of CPU time have already been used) or the development of some new simulation or data analysis methods.

Several studies have also shown that other models that undergo second-order transitions in the pure system apparently have Ising critical behavior when impurities are present [3]. It is interesting that system with quenched randomness, site or bond, appear to be in the same universality class of a pure 2D Ising model, although there is insufficient accuracy to say anything about possible logarithmic corrections. In contrast, simulations of the $q=8$ ferromagnetic Potts model on random 2D lattices show strong evidence for a first-order transition [45]. We know of no theoretical prediction for the anticipated critical behavior in this bond impure model and would encourage theoretical effort to explain it.

ACKNOWLEDGMENTS

This work was supported in part by NSF Grants Nos. DMR-9100692 and DMR-9405018.

APPENDIX: THE DOUBLE-PEAKED STRUCTURE IN THE SPECIFIC HEAT

In analyzing the specific heat for $r=10$, we found that the specific heat for some of the bond configurations has two peaks (Fig. 10). The maximum can be either one of the peaks depending on the bond distribution. Without foreknowledge of the location of the phase transition, it is impossible to determine which peak signals the phase transition for that particular configuration. The work shown in this appendix will provide an understanding of the double-peaked structure of the specific heat by the systematic study of a two-bond system without randomness.

The idea is that instead of choosing K_{ij} "randomly" from K_1 and K_2, we assign them periodically so that the variation of the amplitudes and locations of the peaks with bond configuration can be observed systematically. Two types of bond configurations, "strip" and "square," have been studied. Examples are shown in Figs. 11(a) and 11(b), where solid and dotted lines represent strong and weak bonds, respectively. L is the number of bonds in each direction and W is the number of strong or weak

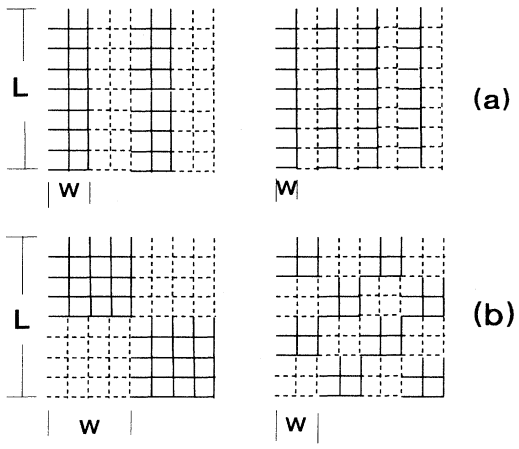

FIG. 11. Plot of an example of the periodic, regularly formed bond configurations, where solid and dashed lines represent strong and weak bonds, respectively. L is the linear size of the lattice and W is the width of the strip domain or the linear size of the square domain.

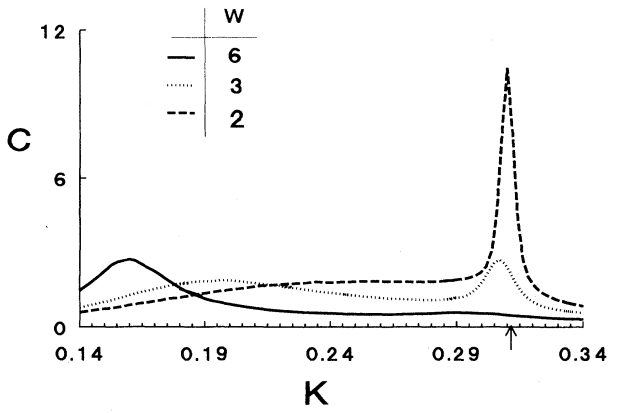

FIG. 12. Coupling dependence of the specific heat for various size square domains with lattice size $L=36$. The arrow shows the location of the exact transition point ($K_{1c}=0.312\,655\ldots$) for the random system with $r=10$.

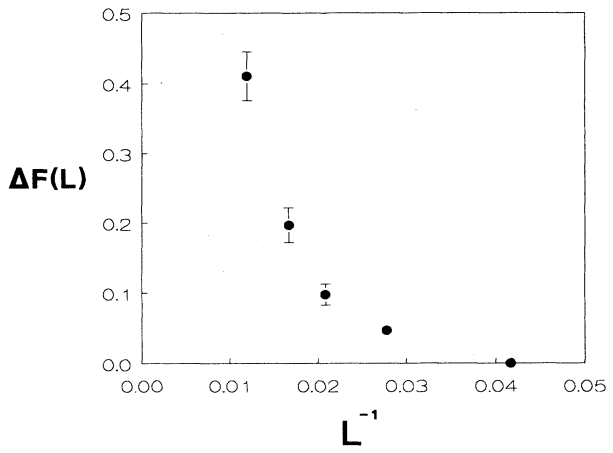

FIG. 14. Plot of the free-energy barrier $\Delta F(L)$ as a function of inverse lattice size for 3×3 square domain bond configurations.

bonds in one period. Monte Carlo simulations were then performed over wide range of couplings for the $q=8$ Potts model with the arranged bond configuration. We first observe the specific heat for the strip configuration with only two regions, one with strong (coupling constant $J=10$) and one with weak ($J=1$) bonds. The result shows that the specific heat has two peaks with the amplitude of each peak increasing with lattice size. Intuitively, we could expect that when the size of each strip approaches infinity, the influence of the interface becomes relatively small, thus each domain (containing the same type of bonds) approaches its own thermodynamic limit properties, undergoing a first-order transition.

Second, we investigate the specific heat in the square [Fig. 11(b)] bond configuration, which has more interfaces of strong and weak bonds compared to the two-strip configuration. In Fig. 12 we plot the coupling dependence of the specific heat for $L=36$ with various W.

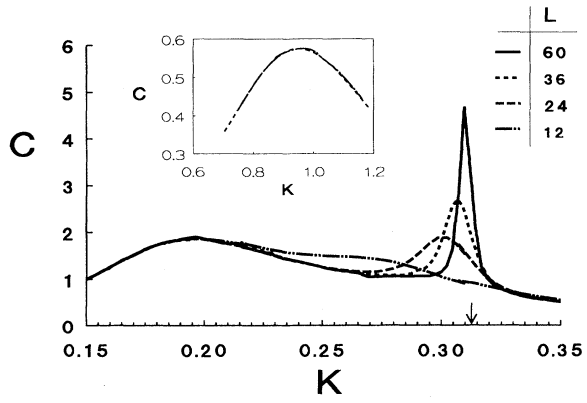

FIG. 13. Coupling dependence of the specific heat for various lattice sizes for a 3×3 square domain bond configuration. The arrow shows the location of the exact transition point of the random system with $r=10$. The figure in the top box shows the coupling dependence of specific heat at high coupling side.

With increasing interfaces of strong and weak bonds or, in other words, decreasing W, the peaks move from the infinite-lattice transition points K_{J_1} and $K_{J_{10}}$, respectively, to the transition point $K_{r_{10}}=0.312\,66\ldots$ of the random system with decreasing amplitudes. A third peak has been observed in the position near $K_{r_{10}}$, which was not found in the two-strip configuration. When the width of the squares is one, only one peak is observed. The absence of the third peak in the two-strip configuration suggests that this peak is present only when the system contains enough interfaces between "domains" of strong and weak bonds and the width of the domain that contains same type of coupling constant is not too large. It is very likely that the third peak is the one signaling the phase transition in the random system. Again, only one peak is observed when the width of the domain is one.

Finally, to study finite-size effects we observed how the specific heat varied with system size for a square configuration [Fig. 11(b)] with constant width ($W=3$). The result is shown in Fig. 13. It is clear that only the middle peak increases with system size. The other two peaks, which are indeed characteristic of the short-order correlation length of a particular bond distribution, do not increase with lattice size when W is invariant. Fitting the specific heat for large lattices to a power law, we find that α/ν is very nearly equal to 2, the value it would take at a first-order transition. Further confirmation of this can be seen in Fig. 14, which shows that the Lee-Kosterlitz free-energy barrier is increasing rapidly with system size.

Our observations suggest that the local collection of distinct bond domains might be responsible for the multiple-peak phenomena in the specific heat, which happens in the periodically arranged or random-bond system. However, the nature of the phase transition of the periodically arranged bond system remains first order, suggesting that it is the "randomness" that induces the second-order phase transition.

[1] A. B. Harris, J. Phys. C **7**, 1671 (1974).
[2] A. Aharony, Phys. Rev. B **18**, 3318 (1978).
[3] Simulation studies of impure Ising models are reviewed in W. Selke, in *Computer Simulation Studies in Condensed Matter Physics, IV,* edited by D. P. Landau, K. K. Mon, and H.-B. Schüttler (Springer-Verlag, Heidelberg, 1993); results for the site impure Baxter model are given in D. Matthews-Morgan, D. P. Landau, and R. H. Swendsen, Phys. Rev. Lett. **53**, 679 (1984), and for the site impure Baxter-Wu model in M. A. Novotny and D. P. Landau, Phys. Rev. B **24**, 1468 (1981).
[4] Y. Imry and S.-k. Ma, Phys. Rev. Lett. **35**, 1399 (1975).
[5] G. Grinstein and S.-k. Ma, Phys. Rev. Lett. **49**, 684 (1982).
[6] A. N. Berker, Phys. Rev. B **29**, 5293 (1984).
[7] K. Hui and A. N. Berker, Bull. Am. Phys. Soc. **33**, 813 (1988).
[8] S. Trimper, Phys. Lett. **113A**, 45 (1985).
[9] K. Hui and A. N. Berker, Phys. Rev. Lett. **62**, 2507 (1989); **63**, 2433(E) (1989).
[10] A. Aizenman and J. Wehr, Phys. Rev. Lett. **62**, 2503 (1989).
[11] A. N. Berker and K. Hui, in *Science and Technology of Nanostructured Magnetic Materials,* edited by G. C. Hadjipanayis, G. Prinz, and L. Paretti (Plenum, New York, 1991).
[12] F. Y. Wu, Rev. Mod. Phys. Rev. **54**, 235 (1982).
[13] R. J. Baxter, H. N. V. Temperley, and S. E. Ashley, Proc. R. Soc. London A **358**, 535 (1978).
[14] See *Finite Size Scaling and Numerical Simulation of Statistical* Systems, edited by V. Privman (World Scientific, Singapore, 1990); K. Binder, in *Phase Transitions and Critical Phenomena,* edited by C. Domb and M. S. Green (Academic, New York, 1976), Vol. 5b; in *Monte Carlo Methods in Statistical Physics,* edited by K. Binder (Springer, New York, 1979), M. N. Barber, in *Phase Transitions and Critical Phenomena,* edited by C. Domb and J. L. Lebowitz (Academic, New York, 1983), Vol. 8.
[15] J. Lee and J. M. Kosterlitz, Phys. Rev. Lett. **65**, 137 (1990).
[16] F. Y. Wu and Y. K. Wang, J. Math. Phys. **17**, 439 (1976).
[17] W. Kinzel and E. Domany, Phys. Rev. B **23**, 3421 (1981).
[18] J. S. Wang and R. H. Swendsen, Physica A **167**, 520 (1990).
[19] S. Chen, A. M. Ferrenberg, and D. P. Landau, in *Computer Simulation Studies in Condensed Matter Physics IV,* (Ref. [3]).
[20] R. H. Swendsen and J.-S. Wang, Phys. Rev. Lett. **58**, 86 (1987).
[21] H. Mino, Comput. Phys. Commun. **60**, 25 (1991).
[22] A. M. Ferrenberg and R. H. Swendsen, Phys. Rev. Lett. **61**, 2635 (1988).
[23] A. M. Ferrenberg and R. H. Swendsen, Phys. Rev. Lett. **63**, 1195 (1989).
[24] A. M. Ferrenberg, D. P. Landau, and R. H. Swendsen, Phys. Rev. E **51**, 5092 (1995).
[25] J. Dongarra, G. A. Geist, R. Monchek, and V. S. Sunderam, Comput. Phys. **7**, 166 (1993).
[26] N. A. Alves, B. A. Berg, and R. Villanova, Phys. Rev. B **41**, 383 (1990).
[27] A. M. Ferrenberg and D. P. Landau, Phys. Rev. B **44**, 5081 (1991).
[28] A. M. Ferrenberg, in *Computer Simulation Studies in Condensed Matter Physics, III,* edited by D. P. Landau, K. K. Mon, and H.-B. Schüttler (Springer-Verlag, Heidelberg, 1991).
[29] M. E. Fisher, in *Critical Phenomena,* edited by M. S. Green (Academic, New York, 1971); M. E. Fisher and M. N. Barber, Phys. Rev. Lett. **28**, 1516 (1972).
[30] F. J. Wegner, Phys. Rev. B **5**, 4529 (1972).
[31] M. E. Fisher and A. N. Berker, Phys. Rev. B **26**, 2507 (1982).
[32] J. L. Cardy and M. P. Nightingale, Phys. Rev. B **27**, 4256 (1983).
[33] K. Binder and D. P. Landau, Phys. Rev. B **30**, 1477 (1984).
[34] J. Lee and J. M. Kosterlitz, Phys. Rev. B **43**, 3265 (1991).
[35] M. S. S. Challa, D. P. Landau, and K. Binder, Phys. Rev. B **34**, 1841 (1986).
[36] K. Binder, Rep. Prog. Phys. **50**, 783 (1987).
[37] C. Borgs and W. Janke, Phys. Rev. Lett. **68**, 1738 (1992).
[38] C. Borgs and R. Kotecky, Phys. A **194**, 128 (1993).
[39] A. Billoire, R. Lacaze, and A. Morel, Nucl. Phys. B **370**, 773 (1992).
[40] K. Vollmayr, J. D. Reger, M. Scheucher, and K. Binder, Z. Phys. B **91**, 113 (1993).
[41] A. Hüller, Z. Phys. B **95**, 63 (1994).
[42] A similar suggestion was made in K. Binder, Z. Phys. B **43**, 119 (1981).
[43] S. Chen, A. M. Ferrenberg, and D. P. Landau, Phys. Rev. Lett. **69**, 1213 (1992).
[44] W. Janke, in *Computer Simulation Studies in Condensed Matter Physics, VII,* edited by D. P. Landau, K. K. Mon, and H.-B. Schüttler (Springer-Verlag, Heidelberg, 1994); C. Borgs and W. Janke, J. Phys. (France) I **2**, 2011 (1992).
[45] W. Janke (private communication).